



Highly sensitive detection of proteins using voltammetric assay in the presence of silver nanostructures

Loganathan Bhavani Devi^a, Sheela Berchmans^b, Asit Baran Mandal^{a,*}

^aChemical Laboratory, CSIR – Central Leather Research Institute, Chennai 600 020, India

^bEEC Division, CSIR – Central Electrochemical Research Institute, Karaikudi 600 036, India

ARTICLE INFO

Article history:

Received 4 August 2011

Received in revised form 8 November 2011

Accepted 11 November 2011

Available online 22 November 2011

Keywords:

Voltammetric assay

Self-assembly

Nanostructures

BSA

Adsorption

ABSTRACT

A novel voltammetric protein assay has been demonstrated using bovine serum albumin in the presence of silver nanostructures (AgNs) formed electrochemically on gold substrates modified by self-assembled monolayer of thioctic acid. It is shown that the prepared AgNs exhibit voltammetric response characteristic of Ag and shows near Nernstian response at physiological pH. The advantages of the electrochemical assay compared to conventional protein analysis are the wide linear concentration range (10^{-4} – 10^{-11} g/mL) and trace level detection limits (50 pg/mL). The result of this electrochemical analysis agreed well with an independent spectrophotometric method using Bradford reagent, but the detection limit is far superior using the electrochemical method. Further, the modified electrode exhibits high sensitivity and long term stability. We invoke a new concept of surface enhanced activity of Ag^+ ions at the electrochemical interface by the negatively charged bovine serum molecules.

© 2011 Elsevier B.V. All rights reserved.

1. Introduction

In recent years, there has an increasing interest in the design and development of silver nanomaterial for biological and bioanalytical applications, since it possesses biocompatibility and low toxicity. The size, shape, morphology and structure of nanomaterials play important roles in the modulation of electronic and optical properties. Silver based nanomaterials have been prepared in several shapes such as nanoparticles, nanoplates, and nanoprisms [1–3]. Due to their unique physical, chemical, and mechanical properties, silver nanomaterials hold much promise for applications in catalysis [4], surface-enhanced Raman scattering (SERS) as excellent substrates [5–7], DNA sequencing [8], sensors [9–11], etc. Recently, the electrocatalytic activity of Ag has been investigated [12,13]. These nanostructured noble metal surfaces and colloidal NPs have been employed for protein characterization and detection [14–20]. The detection of proteins is critically important in many fields due its application [21,22]. SERS based protein detection using Coomassie brilliant blue G-250 (CBBG) dye has been developed [23].

Protein assay is a basic biochemical method and often necessary before processing protein samples. The most commonly used ways to determine protein concentration are the Bradford, Lowry and BCA methods. These methods, however, have definite limitations

with respect to sensitivity, dynamic range and compatibility with reducing agents [24]. Amongst all methods, Bradford has been used for its rapidness, convenience and relative sensitivity. This protein assay is based on absorbance shift from 465 to 595 nm of a band arising from CBBG when binding to proteins occurs in an acidic solution. The disadvantage of the Bradford assay is, however, its narrower linear concentration range (0.2–20 $\mu\text{g/mL}$), which presents a severe problem when the concentration of a target protein is outside the range [25–27]. One of the way to overcome the disadvantage of Bradford assay is the use of electrochemical method to determine protein concentration. Cyclic voltammetry is the simplest electrochemical method used to detect various analytes of interest [28–33] and to calculate extent of binding of substrate to biomolecules [34,35]. As an ultrasensitive and promising analytical tool, this technique is widely applied to various quantitative analyses, for instance, investigations of adsorption, orientation, and electron transfer of molecules on a metal surface [36–39]. For the past decade, determination of proteins using cyclic voltammetry has been extensively studied [40,41]. Bovine Serum Albumin (BSA) is one of the serum albumin proteins that has enormous biochemical applications. The detection of BSA has become wide area of research in immunology and bioanalytical studies [42,43]. Hence in the present study, we have developed a novel voltammetry-based method for the label-free detection of proteins using BSA in presence of electrochemically formed silver nanostructures (AgNs) on Au substrates modified by a self assembled monolayer (SAM) of thioctic acid (TA).

* Corresponding author. Tel.: +91 44 2491 0846/0897; fax: +91 44 2491 2150.
E-mail address: abmandal@hotmail.com (A.B. Mandal).

2. Experimental

2.1. Materials and methods

AgNO₃, CuSO₄, thioctic acid and BSA were purchased from Sigma Aldrich. All solutions were prepared using double distilled water and experiments were carried out at ambient temperature. Phosphate buffer (10 mM) was used to prepare BSA solution. Gold slides (1000 Å Au coating on Si wafers with an intermediate adhesion layer of 100 Å thick Ti, procured from Lance Goddard Associates, USA) of size 1 × 1 cm² were used in XPS and SEM measurements. The geometric area of the working electrode was 15.07 × 10⁻² cm². It was washed thoroughly with distilled water and immediately conditioned in H₂SO₄ (0.5 M) from *E* = 0.0–1.5 V for at least ten complete scans at 50 mV s⁻¹ until reproducible cyclic voltammograms were established.

The morphology and oxidation state of AgNs were characterized using Hitachi S3000-H scanning electron microscope (SEM) and Omicron nanotechnology X-ray Photoelectron Spectrometer (XPS). Voltammograms were recorded using PARSTAT 2263. A conventional three-electrode cell was used, with a gold slide, as the working electrode, Hg|Hg₂SO₄|0.5MH₂SO₄ (MMS) or Hg|Hg₂Cl₂|1NKCl (NCE) as reference electrode and a Pt wire as the counter electrode.

2.2. Preparation of silver nanostructure

AgNs was prepared by using Au (111) substrate immersed in a saturated solution of TA in ethanol for 30–36 h [44]. After incubation in TA solution, Au slides were washed with ethanol, air-dried, and then immersed in a 1 mM CuSO₄ solution for 20 min for chemical pre-concentration of Cu²⁺ ions on the SAM of TA. After the pre-concentration, the substrate was taken out of the solution, washed with water, and then introduced into a cell containing 0.5 M H₂SO₄ for electrochemically reducing the Cu²⁺ ions trapped by the monolayer of TA. The working electrode was clamped at a potential of -600 mV that is sufficient to reduce the Cu²⁺ ions. The Cu adlayer formed was then galvanically replaced by Ag by immersion in an aqueous solution of AgNO₃ (1 mM) for 20 min. The prepared film was cycled in the potential range of -0.6 to 0.6 V in 0.5 M H₂SO₄ [45].

3. Results and discussion

3.1. Characterization of AgNs-modified Au electrode

AgNs was characterized using EDAX, XPS and SEM. EDAX analysis (Fig. 1) proved that surface coated nanostructures were silver. Furthermore, XPS was used to confirm the oxidation state of Ag that was deposited on modified electrode. XPS spectrum of AgNs was illustrated in Fig. 2. The peaks centered at binding energy of 368 and 374 eV can be ascribed to Ag 3d_{5/2} and Ag 3d_{3/2}, respectively. These binding energy values were in agreement with the metallic silver [46]. This ensured that the prepared AgNs possess zero oxidation state in the absence of applied potential.

The morphology of AgNs was studied using scanning electron microscope (SEM). Fig. 3 shows a typical SEM image of AgNs/Au. From the micrograph, it was observed that AgNs deposited with the size range 90–160 nm and histogram of the nanostructure with respect to size was reported.

The formation of AgNs on the electrode surface was verified by recording cyclic voltammogram (CV) of the modified electrode (AgNs/Au) in 0.5 M H₂SO₄ (Fig. S1). A sharp oxidation peak at 0.075 V vs. MMS confirms the formation of AgNs, which can be attributed to the oxidation of Ag(0) to Ag¹⁺. AgNs thus deposited exhibits irreversible nature in acid medium. According to Laviron theory, the transfer coefficient (α) and electron transfer rate constant (*k*) can be estimated by measuring variation of peak potential with the scan rate [47].

$$\log k = \alpha \log(1 - \alpha) + (1 - \alpha) \log \alpha - \log(RT/nFv) - \alpha(1 - \alpha)nF\Delta E_p/2.3RT \quad (1)$$

where *k* heterogenous electron transfer rate constant, α transfer coefficient, *F* Faraday constant, *v* scan rate, *R* gas constant. From Eq. (1), *k* of AgNs was calculated to be 1.33 s⁻¹ and the electron transfer was found to be diffusion-controlled.

CV of AgNs/Au in 0.01 M phosphate buffer (PB) at different scan rates was shown in Fig. 4. A pair of redox peak was observed at 0.19 and -0.032 V vs. NCE, which was ascribed to the redox of silver. The peak potential (*E_p*) was proportional to logarithm of scan rate in the range 30–200 mV/s and the peak current increased with increase in scan rate (inset a of Fig. 4). The separation of anodic to cathodic peak potential (ΔE_p) was >200 mV and the ratio of *i_{pa}*/*i_{pc}*

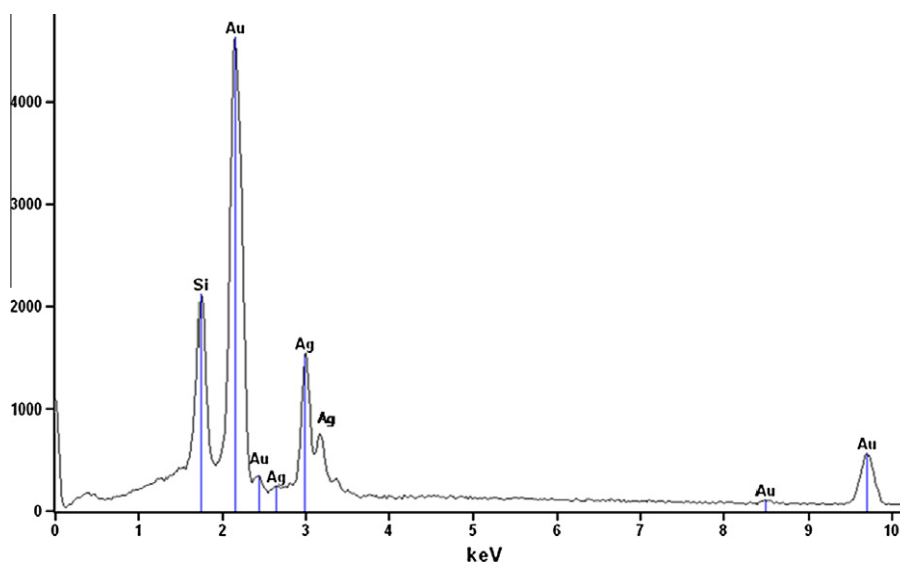


Fig. 1. EDAX of AgNs deposited on the modified electrode (Au and Si peaks correspond to substrate).

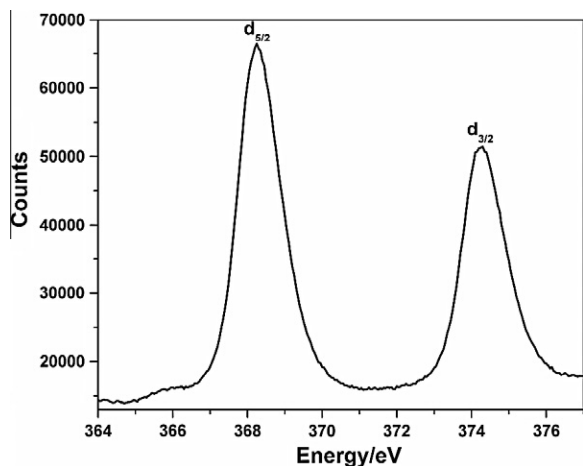


Fig. 2. XPS spectrum of AgNs on the modified electrode.

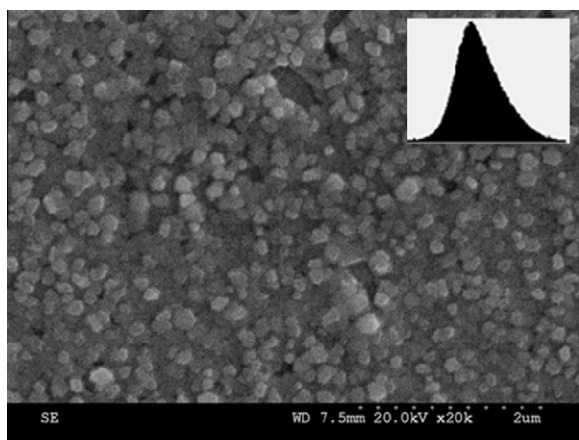


Fig. 3. SEM image of AgNs on the modified electrode.

was found to be unity. This indicates that AgNs undergoes a quasi-reversible redox process. The irreversible behavior of AgNs in the presence of H_2SO_4 might be due to the interaction of Ag ions with sulfate anions which is absent in the case of phosphate buffer. Therefore, it was clearly seen from CV that AgNs/Au exhibits irreversible nature in acid medium while it undergoes quasi-reversible process in physiological pH. Also physiological pH is compatible for the determination of biological analytes and will not induce any adverse effect in protein.

To obtain the kinetic parameters of AgNs/Au, scan rate effect was investigated. The inset of Fig. 4b shows that the cathodic and anodic peak currents were proportional to $v^{1/2}$, suggest that the electrochemical reaction of Ag modified electrode is a diffusion-controlled process. The heterogeneous electron transfer rate constant was calculated to be $0.6054 s^{-1}$. The observed k^0 was higher than the reported value of $8.4 \times 10^{-6} s^{-1}$ [48]. This enhanced value shows that the electron transfer at AgNs/Au is more facile.

In order to calculate the surface concentration (Γ_c) of Ag on AgNs/Au Eq. (2) was used. From the plot of peak current vs. scan rate, Γ_c was determined.

$$I_p = n^2 F^2 A \Gamma_c v / 4RT \quad (2)$$

where n is the number of electrons, F Faraday constant, A is the effective surface area, v is the sweep rate, Γ surface concentration

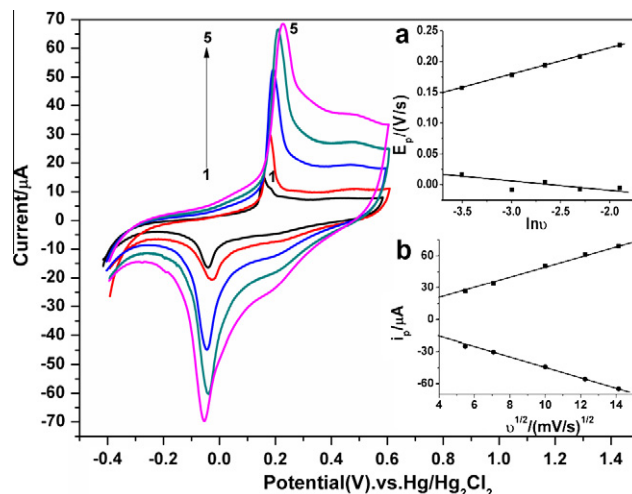


Fig. 4. CV of AgNs/Au in 0.01 M PB (pH 7) at different scan rates. Curve nos. (1–5): 30, 70, 100, 150 and 200 mV/s respectively. Inset (a) is plot of E_p vs. $\ln v$. Inset (b) is linear relationship of i_p and $(v)^{1/2}$.

of the electroactive species, R gas constant. The calculated surface concentration of Ag was found to be $2.54 \times 10^{-10} mol/cm^2$, indicating monolayer formation of Ag on modified Au electrode.

3.2. Stability of AgNs modified film

Long term stability is one of the most important properties for sensors. The peak height and peak potential of the surface immobilized film remained nearly unchanged when subjected to potential cycling over the range of -0.4 to 0.4 V. The amount of Ag remaining on the electrode surface was almost 99% of its initial value after been used for 100 repetitive cycles with fresh solution. Thus, high stability of modified electrode was related to the chemical stability of Ag film. Therefore, AgNs/Au electrode can be used as a sensing matrix due to its long term stability and excellent electron transfer rate constant.

3.3. Determination of BSA using AgNs/Au

As an application of AgNs in bioanalytical techniques, the modified electrode was used for the determination of proteins using BSA. Herein, we have investigated the ability of AgNs to determine the concentration of BSA over a wide range.

Fig. 5 shows the comparison of CV of bare Au electrode and AgNs/Au in the presence of BSA. From Fig. 5 it was seen that there was significant increase in peak current with the addition of BSA in the case of AgNs rather than bare Au electrode. The addition of BSA to the PB solution resulted in a change in voltammetric response. However, the profile of CV remains unaltered but the resulting current, i.e. charge, increased considerably. This proves the interaction of protein molecules with Ag surface. Oxidation of the proteins could be excluded as a reason for the observed increase of the charge, since the measurements were done in a low cathodic potential region. Since the shape of the voltammogram remained essentially the same after addition of BSA, the observed increase in charge could be due to strong electrostatic attraction between positively charged AgNs and negatively charged BSA at the applied potential.

At pH 7, which is greater than isoelectric point of BSA, the carboxyl groups in BSA molecule carry a negative charge. In addition, Ag surface has a net positive charge in the investigated potential region, which facilitates the involvement of these negatively charged carboxyl groups of the proteins as anchoring sites in the

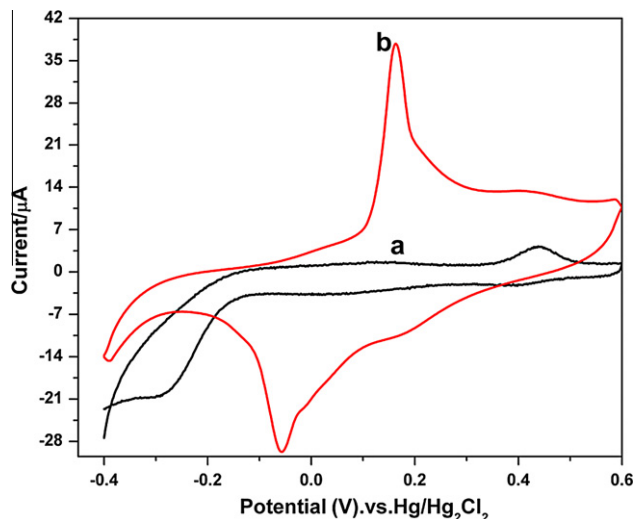


Fig. 5. CVs of AgNs/Au in PB (pH 7) in the (a) absence of BSA and (b) presence of BSA; scan rate 50 mV/s; [BSA] = 0.5 nM.

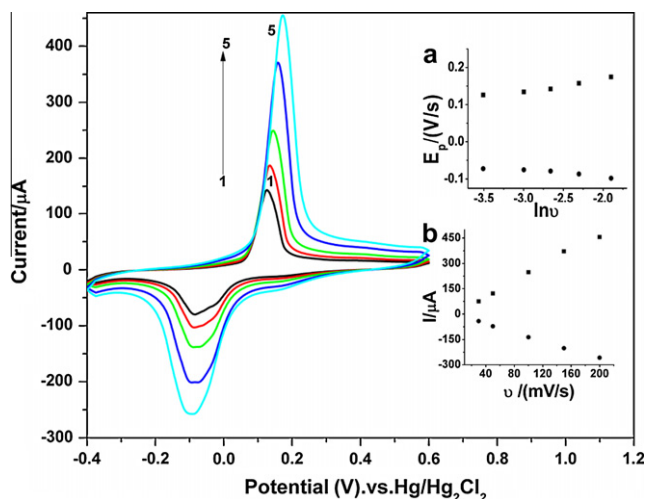


Fig. 6. CV curves of AgNs in 0.01 M PB (pH 7) at different scan rates on AgNs/Au in the presence of BSA. Scan rate: 30, 70, 100, 150 and 200 mV/s respectively. Inset (a) is plot of E_p vs. $\ln \nu$. Inset (b) is linear relationship of i_p and ν at AgNs/Au.

contact region [49]. Further, in the presence of BSA the activity of Ag ion increases. This increase is mainly due to the oxidation current of Ag and the strong interaction between Ag ion and BSA. In the absence of BSA, the activity of Ag^0 that can undergo oxidation is less since it is strongly bound to the interface. In the presence of negatively charged BSA, the activity of Ag^0 that can get oxidized

increases and therefore, the current proportionally increases with the addition of BSA. We can call this effect as “surface enhanced activity” of Ag induced by BSA.

The CVs for BSA/Ag were studied at different scan rates in the range of 30–200 mV/s shown in Fig. 6. The cathodic current was slightly perturbed while anodic current was enhanced and i_{pa}/i_{pc} was greater than unity. Plot of E_p vs. $\ln \nu$ (Fig. 6a) shows that peak potential was proportional to scan rate. But the wave was shifted positively from the reversible value and was distorted from its symmetrical shape, representing a decrease in dissolved BSA near the electrode surface because of adsorption. The peak current varies linearly with ν as shown in inset b of Fig. 6 with correlation coefficient 0.9943. The peak current value is given by Eq. (3) from which heterogeneous rate constant, k can be calculated [50].

$$I_p = 0.227 \text{ FAC}_0^* k e^{-\alpha f \Delta E_{p,1/2}} \quad (3)$$

Using Eq. (3), the rate constant value was estimated as $1.14 \times 10^{-3} \text{ s}^{-1}$ which was less than that of AgNs/Au. This decrease in k proves that electro-inactive complex was formed as a result of interaction of BSA with AgNs. Further plot of i_p vs. ν shows that interaction of BSA with AgNs was surface controlled process.

Fig. 7 shows micrograph obtained from AgNs in the presence of BSA. From the SEM images, we can observe that the aggregate formation was distinctly different. The negatively charged BSA forms aggregates at high concentration (10^{-4} g/mL), which may be due to their interactions with positively charged AgNs, while aggregation was not favoured at low concentration.

Voltammogram of AgNs with increasing [BSA] for two different ranges (5×10^{-6} – 10^{-4} g/mL (Fig. 8) and 10^{-11} – $5 \times 10^{-6} \text{ g/mL}$ (Fig. 9)) indicate that peak current increased linearly with increase in [BSA] and the calibration plot was linear ($r^2 = 0.9991$) for a wide range of concentration. The detection limit of the assay towards BSA detection was found to be 50 pg/mL. The proposed method was applied to determine unknown protein concentration and the results were compared with that obtained by Bradford method (inset b of Fig 8). The result shows that detection using CV provides better sensitivity. When compared to Bradford method, the values obtained by this method are within 1–2% error. Therefore, the detection method of proteins by this new electrochemical method is reliable, practical and reproducible with high sensitivity.

3.4. Kinetics of albumin adsorption

A number of studies have been made on the interaction of proteins with metal surfaces to determine the molecular conformation or orientation of the adsorbed molecules. The surface charge density resulting from protein adsorption was found to be sensitive to the conformational behavior of the proteins. In this work, to identify the adsorption characteristics of BSA on AgNs, we have determined saturated surface coverages and thermodynamic adsorption values of BSA on AgNs. Langmuir Equation provides a

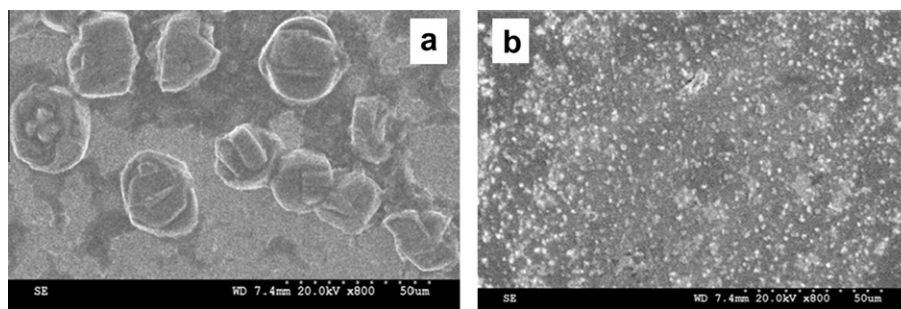


Fig. 7. A&B SEM images of BSA/AgNs/Au high concentration 10^{-4} g/mL and low concentration 10^{-8} g/mL .

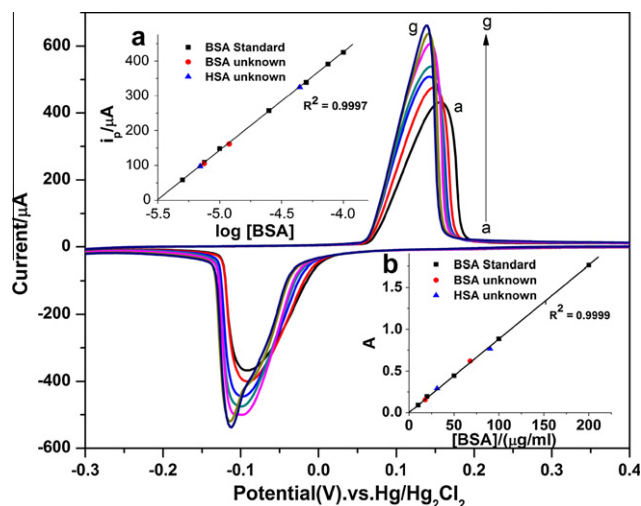


Fig. 8. CV of AgNs/Au in 0.01 M PB in the presence of BSA, Scan rate: 50 mV/s, pH 7.0; Curve nos. (a–g): [BSA] = 0.05, 0.075, 0.1, 0.25, 0.5, 0.75 and 1×10^{-4} g/mL, respectively. Inset plot (a) i_p vs. $\log[\text{BSA}]$ and (b) Bradford method: A vs. [BSA].

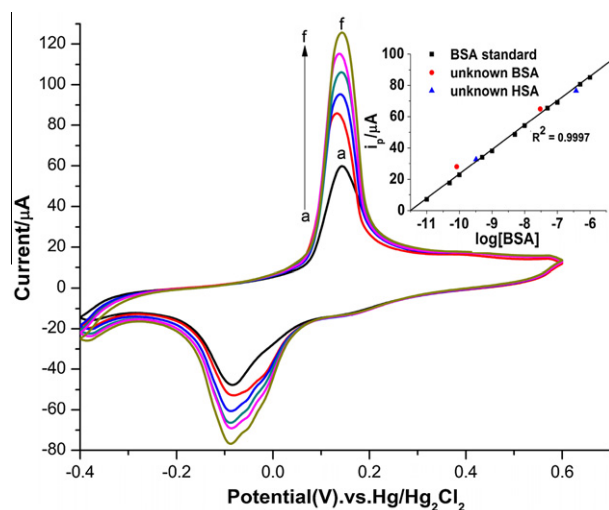


Fig. 9. CV of AgNs/Au in 0.01 M PB in the presence of BSA (pH 7), Scan rate 50 mV/s, Curve nos. (a–f): [BSA] = 10^{-11} , 10^{-10} , 10^{-9} , 10^{-8} , 10^{-7} and 5×10^{-6} g/mL, respectively.

relationship between the concentration of the protein in solution, c , and the amount of material adsorbed on the surface:

$$c/\Gamma = 1/B_{\text{ADS}}\Gamma_{\text{MAX}} + c/\Gamma_{\text{MAX}} \quad (4)$$

where B_{ADS} is the adsorption coefficient which reflects the affinity of the adsorbate molecules towards adsorption sites at a constant temperature and Γ_{MAX} represents the maximum amount of material that can adsorb on the surface. Plotting c/Γ vs. c yields a straight line and Γ_{MAX} and B_{ADS} can be derived from the slope and intercept, respectively. This value can be related to the Gibbs energy of adsorption, ΔG_{ADS} through

$$B_{\text{ADS}} = \frac{1}{55.5} \exp\left(\frac{-\Delta G_{\text{ADS}}}{RT}\right) \quad (5)$$

where 55.5 represents the molar concentration of water (mol/L), which was used as the solvent. From the analysis of the kinetics of albumin adsorption, we can conclude that full coverage of BSA was attainable on AgNs. The data obtained for adsorption of BSA on AgNs/Au from 8×10^{-5} M BSA solution was presented in Table

Table 1
Adsorption data of BSA on AgNs.

Parameter	Data
Molecular weight (kDa)	66,000
B_{ADS} (l/mol)	8.6×10^6
ΔG_{ADS} (kJ/mol)	-49.5
Γ_{MAX} (mol/cm ²)	3.75×10^{-10}
Γ_{MAX} (mg/m ²)	247
Q_{MAX} (C/cm ²)	3.85×10^{-5}

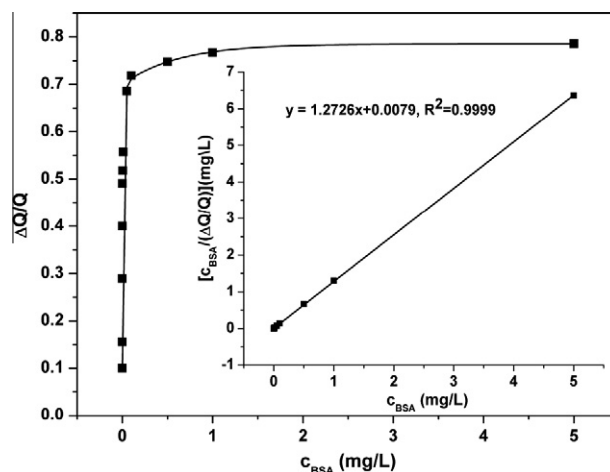


Fig. 10. Increase in the integrated charge (reduction peak) as a function of concentration of BSA (experimental condition same as Fig. 8 and 9) Inset is linearized adsorption isotherm of BSA binding to AgNs based on the Langmuir model. The line is the best linear fit to the experimental data.

1. The total mass of BSA adsorbed on Ag modified electrode was found to be 247 mg m^{-2} or $3.74 \times 10^{-10} \text{ mol/cm}^2$ which was higher than that of the theoretical monolayer surface coverage of BSA (6.7 mg/m^2) [51]. This indicates multilayer formation of BSA film on AgNs/Au at the concentration 8×10^{-5} M BSA. In addition, $-\Delta G^0$ confirmed the spontaneous adsorption of negatively charged BSA onto positively charged AgNs.

To calculate how efficient the adsorption of BSA to AgNs, Langmuir adsorption isotherm was used. It is well known that the adsorption isotherm of BSA binding to AgNs can be regarded as arising from electrostatic interaction of proteins with AgNs. Based on the classical Langmuir model, a linearized form of the adsorption isotherm is shown:

$$\frac{c}{\Delta Q/Q} = \frac{c}{(\Delta Q/Q)_{\text{sat}}} + \frac{K_D}{(\Delta Q/Q)_{\text{sat}}} \quad (6)$$

in which c is the concentration of BSA in solution, $\Delta Q/Q$ is the sensor signal, $(\Delta Q/Q)_{\text{sat}}$ is the saturated sensor signal, and K_D is the dissociation constant. The dependence of the relative increase in the charges obtained by integration of the oxidation peak of AgNs in the CVs before and after the addition of BSA is given by, $\Delta Q/Q = |(Q - Q_i)/Q|$ (where Q and Q_i denote, respectively, the charges obtained before and after addition of different concentration of BSA). As shown in Fig. 10 inset, the experimental results for $c/(\Delta Q/Q)$ are in an almost perfect linear relationship over the range 10^{-11} – 10^{-4} g/L BSA with $r^2 = 0.9999$. Based on the linear fit of the above equation, the K_D of AgNs and BSA can be calculated as 6.2×10^{-3} M which indicates the adsorption of protein onto the surface of AgNs. Additionally, this AgNs-modified sensor has a very low detection limit of 50 pg/mL.

4. Conclusion

We have developed a CV-based method for the determination of protein concentration using cyclic voltammetry rather than the absorbance measurements like Bradford protein assay. The prepared AgNs possess high electron transfer rate constant of almost five orders of magnitude than the reported value and hence it may be used as excellent SERS substrate. The differences in peak current are significant even for low concentration such as 0.1 pM. The proposed method facilitates one to determine protein concentrations over a much wider linear concentration range with a lower limit of detection than currently used protein assays. This voltammetric based protein assay exhibits high sensitivity, good reproducibility, and long-term stability which may have potential applications in future.

Acknowledgements

This work was supported by CSIR. One of the authors Sheela Berchmans acknowledge the funding received from the CSIR network Project (NWP0035) for carrying out this work.

Appendix A. Supplementary material

Supplementary data associated with this article can be found, in the online version, at [doi:10.1016/j.jelechem.2011.11.013](https://doi.org/10.1016/j.jelechem.2011.11.013).

References

- [1] G.S. Metraux, C.A. Mirkin, *Adv. Mater.* 17 (2005) 412–415.
- [2] H.H. Huang, X.P. Ni, G.L. Loy, C.H. Chew, K.L. Tan, F.C. Loh, J.F. Deng, G.Q. Xu, *Langmuir* 12 (1996) 909–912.
- [3] Y. Sun, Y. Xia, *Adv. Mater.* 15 (2003) 695–699.
- [4] W. Grunert, A. Bruckner, H. Hofmeister, P. Claus, *J. Phys. Chem. B* 108 (2004) 5709–5717.
- [5] S. Nie, S.R. Emory, *Science* 275 (1997) 1102–1106.
- [6] X.-M. Lin, Y. Cui, Y.-H. Xu, B. Ren, Z.-Q. Tian, *Anal. Bioanal. Chem.* 394 (2009) 1729–1745.
- [7] M. Muniz-Miranda, T. Del Rosso, E. Giorgetti, G. Margheri, G. Ghini, S. Cicchi, *Anal. Bioanal. Chem.* 400 (2011) 361–367.
- [8] Cao, R. Jin, C.A. Mirkin, *J. Am. Chem. Soc.* 123 (2001) 7961–7962.
- [9] F. Wang, R. Yuan, Y. Chai, D. Tang, *Anal. Bioanal. Chem.* 387 (2007) 709–717.
- [10] A. Steinbruck, O. Stranik, A. Csaki, W. Fritzsche, *Anal. Bioanal. Chem.* 401 (2011) 1241–1249.
- [11] Y. Ma, N. Li, C. Yang, X. Yang, *Anal. Bioanal. Chem.* 382 (2005) 1044–1048.
- [12] G. Gao, D. Guo, C. Wang, H. Li, *Electrochem. Commun.* 9 (2007) 1582–1586.
- [13] E. Sanll, H. Celikkan, B. Zuhtu Uysal, M.L. Aksu, *Int. J. Hydrogen Energy* 31 (2006) 1920–1924.
- [14] I. Pavel, E. McCarney, A. Elkhaled, A. Morrill, K. Plaxco, M. Moskovits, *J. Phys. Chem. C* 112 (2008) 4880–4883.
- [15] C. Mustafa, A. Ahmet, Y.M. Muge, K. Mehmet, S. Fikretin, G. Medine, *Appl. Spectrosc.* 62 (2008) 1226–1232.
- [16] S. Ismail, K. Mehmet, S. Fikretin, Y. Dilsad, C. Mustafa, *Appl. Spectrosc.* 63 (2009) 1276–1282.
- [17] I.D.G. Macdonald, W.E. Smith, *Langmuir* 12 (1996) 706–713.
- [18] C.D. Keating, K.M. Kovaleski, M.J. Natan, *J. Phys. Chem. B* 102 (1998) 9404–9413.
- [19] M. Feng, H. Tachikawa, *J. Am. Chem. Soc.* 130 (2008) 7443–7448.
- [20] T.M. Cotton, S.G. Schultz, R.P. Van Duyne, *J. Am. Chem. Soc.* 102 (1980) 7960–7962.
- [21] O.S. Wolfbeis, A. Dürkop, M. Wu, Z. Lin, *Angew. Chem. Int. Ed.* 41 (2002) 4495–4498.
- [22] J. Zhao, G. Chen, L. Zhu, G. Li, *Electrochem. Commun.* 13 (2011) 31–33.
- [23] X.X. Han, Y. Xie, B. Zhao, Y. Ozaki, *Anal. Chem.* 82 (2010) 4325–4328.
- [24] B.J. Olsen, J. Markwell, *Current Protocols in Protein Science*, John Wiley & Sons, Somerset, NJ, 2007.
- [25] T. Zor, Z. Selinger, *Anal. Biochem.* 236 (1996) 302–308.
- [26] M.M. Bradford, *Anal. Biochem.* 72 (1976) 248–254.
- [27] C.M.M. Stoscheck, *Methods Enzymology*, Academic press, 1990.
- [28] J. Yan, Y. Zhou, P. Yu, L. Su, L. Mao, D. Zhang, D. Zhu, *Chem. Commun.* (2008) 4330–4332.
- [29] A. Hermans, R.B. Keithley, J.M. Kita, L.A. Sombers, R.M. Wightman, *Anal. Chem.* 80 (2008) 4040–4048.
- [30] M.K. Zachek, P. Takmakov, B. Moody, R.M. Wightman, G.S. McCarty, *Anal. Chem.* 81 (2009) 6258–6265.
- [31] A.L. Sanford, S.W. Morton, K.L. Whitehouse, H.M. Oara, L.Z. Lugo-Morales, J.G. Roberts, L.A. Sombers, *Anal. Chem.* 82 (2010) 5205–5210.
- [32] K.-J. Huang, D.-J. Niu, J.-Y. Sun, X.-L. Zhu, J.-J. Zhu, *Anal. Bioanal. Chem.* 397 (2010) 3553–3561.
- [33] L. Li, H. Zhao, Z. Chen, X. Mu, L. Guo, *Anal. Bioanal. Chem.* 398 (2010) 563–570.
- [34] K. Zhong, J. Xia, W. Wei, Y. Hu, H. Tao, W. Liu, *Anal. Bioanal. Chem.* 381 (2005) 1552–1557.
- [35] A. Turcanu, C. Fitz-Binder, T. Bechtold, *J. Electron. Anal. Chem.* 654 (2011) 29–37.
- [36] A.B. Mandal, *Langmuir* 9 (1993) 1932–1933.
- [37] A.B. Mandal, B. Geetha, *Langmuir* 11 (1995) 1464–1467.
- [38] A.B. Mandal, B. Geetha, *Langmuir* 13 (1997) 2410–2414.
- [39] A.B. Mandal, B.U. Nair, *J. Phys. Chem.* 95 (1991) 9008–9013.
- [40] M.F. Smiechowski, V.F. Lvovich, S. Roy, A. Fleischman, W.H. Fissell, A.T. Riga, *Biosens. Bioelectron.* 22 (2006) 670–677.
- [41] L. Fotouhi, S. Banafsheh, M.M. Heravi, *Bioelectrochem.* 77 (2009) 26–30.
- [42] E. Bicer, S. Ozdemir, *J. Electroanal. Chem.* 657 (2011) 128–134.
- [43] W. Sun, K. Jiao, X. Wang, L. Lu, *J. Electroanal. Chem.* 578 (2005) 37–43.
- [44] C. Ramalechume, S. Berchmans, V. Yegnaraman, A.B. Mandal, *J. Electroanal. Chem.* 580 (2005) 122–127.
- [45] P. Arunkumar, S. Berchmans, V. Yegnaraman, *J. Phys. Chem. C* 113 (2009) 8378–8386.
- [46] B. Zhao, Z. Liu, Z. Liu, G. Liu, Z. Li, J. Wang, X. Dong, *Electrochem. Commun.* 11 (2009) 1707–1710.
- [47] E. Laviron, *J. Electroanal. Chem.* 101 (1979) 19–28.
- [48] N. Yang, X. Wang, Q. Wan, *Electrochim. Acta* 52 (2007) 4818–4824.
- [49] D.R. Jackson, S. Omanovic, S.G. Roscoe, *Langmuir* 16 (2000) 5449–5457.
- [50] A.J. Bard, L.R. Faulkner, *Electrochemical Methods*, second ed., Wiley, New York, 2001.
- [51] M. Hepel, *Electroanalysis* 17 (2005) 1401–1412.